



Citation for published version:

Ciampa, F, Pickering, S, Scarselli, G & Meo, M 2014, Nonlinear damage detection in composite structures using bispectral analysis. in Proceedings of SPIE - The International Society for Optical Engineering. vol. 9064.
<https://doi.org/10.1117/12.2046631>

DOI:

[10.1117/12.2046631](https://doi.org/10.1117/12.2046631)

Publication date:

2014

Document Version

Early version, also known as pre-print

[Link to publication](https://doi.org/10.1117/12.2046631)

University of Bath

General rights

Copyright and moral rights for the publications made accessible in the public portal are retained by the authors and/or other copyright owners and it is a condition of accessing publications that users recognise and abide by the legal requirements associated with these rights.

Take down policy

If you believe that this document breaches copyright please contact us providing details, and we will remove access to the work immediately and investigate your claim.

Damage detection and localization in composite structures using nonlinear techniques based on bispectral analysis and radial basis functions

Francesco Ciampa^{*a}, Simon Pickering^a, Gennaro Scarselli^b, Michele Meo^a

^aMaterial Research Centre, Department of Mechanical Engineering,
University of Bath, Bath, BA2 7AY, UK

^bDepartment of Engineering for Innovation, University of Salento,
Via per Monteroni (Lecce), 73100, Italy

ABSTRACT

In different engineering fields there is a strong demand of diagnostic methods able to provide detailed information on the material defects and damages. Indeed, low velocity impact damages can considerably degrade the integrity of structural components and, if not detected, they can result in catastrophic failure conditions. This paper presents a nonlinear Structural Health Monitoring (SHM) method, based on ultrasonic guided waves (GW), for the detection of the nonlinear signature in the dynamic response of a damaged composite structure. The proposed technique is based on a bispectral analysis of ultrasonic waveforms acquired on the structure excited by ultrasounds and allows for the evaluation of the nonlinearities due to the presence of cracks and delaminations. Indeed, such a methodology consists in exploiting the frequency mixing of the original waveform acquired from a sparse array of sensors. The robustness of bispectral analysis was experimentally demonstrated on a damaged carbon fibre reinforce plastic (CFRP) composite panel, and the nonlinear source was retrieved with a high level of accuracy. Unlike other ultrasonic methods for damage detection, this methodology does not require any baseline with the undamaged structure for the evaluation of the damage, nor a priori knowledge of the mechanical properties of the specimen. This technique has been, then, integrated with a radial basis functions approach allowing for an effective visualization of the damage over the panel through an interpolation of the acquired signals. This approach, compared with a conventional imaging technique, has been demonstrated effective in the damage representation also using a limited number of acquisition points.

Keywords: nonlinear elastic wave spectroscopy, bispectral analysis, damage detection, composite materials, radial basis functions.

1. INTRODUCTION

In the aerospace field and in many other engineering applications, Structural Health Monitoring (SHM) based on Non-Destructive Testing techniques attracts the interest of scientists and engineers since it can lead to key information regarding the structural characteristics and the residual life of a component. These methods can provide improved safety and a reduction of maintenance costs. SHM, based on the periodic inspections of the structural integrity of critical components, is becoming more and more reliable, so that damage tolerance criteria play a challenging role in mitigating structural failures due to fatigue in aircraft structural design. The main industrial NDT methods inspect components either by scanning (eddy current, ultrasound) or by using a wide field of view (visual inspection, magnetic particle and penetrant testing) [1], but none is global indeed. A global testing technique allows a component to be tested for damage without attempting to locate the damage, the aim is to allow rapid evaluation of the structural integrity of a component with a single or at most limited measurements for the whole test object. This should allow easy, fast and reliable interpretation of the measurement with a reasonably low effort in terms of hardware and human resources. The effect of damage on the natural frequencies of a sample has been investigated as a potential global inspection technique, but this approach has been proved to be sensitive to environmental factors [2, 3]. The large changes in nonlinear ultrasonic parameters for small degrees of damage [4–6] have stimulated interest in the use of nonlinearity for fatigue crack detection: nonlinear elastic wave spectroscopy (NEWS) shows promise as a route to a sensitive crack detection method.

In [7] ultrasonic waves are used to evaluate the degradation of material properties. The generation mechanism of second-order harmonic frequency components during the propagation of ultrasonic waves through the degraded material is first explained on the basis of nonlinear elasticity. Bispectral analysis as well as power spectral analysis are employed for the evaluation of the nonlinear parameter β , indicating the ratio of the amplitude of second-order harmonic frequency components relative to the power of the fundamental. Several experiments are carried out to confirm the correlation between the values of nonlinear parameter β and the material properties degradation: in particular, β is found proportional to the magnitude of the load and the number of fatigue cycles and reflects the actual variation of the specimen strength well.

In [8] a damage detection investigation carried out using NEWS is presented. The approach is based on the observation of the presence of harmonics and sidebands on the spectrum of acquired signal excited by a bi-tone signal. In absence of damage, the signal spectrum does not present any harmonic or sidebands, which are recorded on the damaged signal spectrum. The harmonic and the sideband amplitudes highlights behavior compatible with the theory. The proposed approach is found capable of detecting the presence of damages on sandwich composite structure, even when this is contained in a small area, and it is hardly visible as for low velocity impact damage.

In [9, 10, 11] the nonlinear elastic wave spectroscopy is applied to several structural samples with the aim of develop robust techniques of detection and localization of the damage. The key factors of these works can be summarized: the monitoring of the generation of harmonics and sidebands to assess the presence of damage; the analysis of the non-linear structural response acquired in different locations of samples in time and frequency domains to evaluate statistical indicators (coherence, bispectrum, bicoherence) able to remark nonlinearities; an algorithm allowing for the visualization of results over the sample in order to localize the damage.

In [12] the use of polyharmonic Radial Basis Functions (RBFs) to reconstruct smooth, manifold surfaces from point-cloud data and to repair incomplete meshes is presented and discussed. An object's surface is defined implicitly as the zero set of an RBF fitted to the given surface data. Fast methods for fitting and evaluating RBFs are presented able to model large data sets, consisting of millions of surface points, by a single RBF. A greedy algorithm in the fitting process is used to reduce the number of RBF centers required to represent a surface, resulting in significant compression and further computational advantages. The energy-minimisation characterisation of polyharmonic splines results in a "smoothest" interpolant. This scale-independent characterisation is well-suited to reconstructing surfaces from nonuniformly sampled data. Holes are smoothly filled and surfaces smoothly extrapolated. A non-interpolating approximation is used when the data is noisy. The functional representation presented in this paper is in effect a solid model, which means that gradients and surface normals can be determined analytically. This helps generate uniform meshes. Furthermore the RBF representation has advantages for mesh simplification and remeshing applications.

This paper presents the use and processing of ultrasounds acquired on a typical panel for aerospace applications in different conditions and the employment of two techniques for imaging the presence of a crack or defect in composite structures. The damage in the sample is imposed through the insertion of a patch in the laminate, influencing the waves propagation. The bispectrum signal processing technique is used to analyze the nonlinear response of the sample to continuous excitation at one frequency properly chosen. The increased nonlinearity due to defect is detected and is quantified by introduction of a parameter, β , based on nonlinear elasticity and measured using bispectral analysis. The acquisition of ultrasonic waves generated in one point of the panel and receiving at different points is performed, then moving the generation point and repeating the test for all the possible combinations receivers/transmitter. A bispectral matrix is generated in this way allowing for the definition of a damage map overlapping the sample formed by discrete values of bispectrum. For the visualization two different approaches have been followed and compared. The results showed a strong correlation of the parameter β and bicoherence with damage in the sample and encouraged the use of nonlinear ultrasonics as structural health monitoring (SHM) technique. The importance of the shape of the excited modes is also demonstrated through the application of the technique in a wide frequency range and suggests that an effective inspection can be achieved only by exciting different modes. The layout of this paper is as follows: in Section 2, bispectral analysis and RBF approach are theoretically presented. Section 3 illustrates the experimental set-up, whilst Section 4 reports the results of the nonlinear imaging process. Finally, conclusions are drawn and summarised.

2. METHOD

In the following section the concepts of bispectrum, second order nonlinear parameter β and bicoherence will be briefly presented and discussed since they represent the theoretical basis of the approach followed in this work for the image of the damage location on the composite structure.

Bispectral Analysis

The most traditional signal processing techniques used to measure the acousto/ultrasonic elastic feature of the medium are the first and second-order statistics, such as mean, variance and power spectrum. Particularly, the last method, which is the decomposition over frequency of the signal power, is related to the auto-correlation function and is mostly designed to describe linear and Gaussian processes. However, power spectral analysis has a drawback of discarding all phase information, and it might not be suitable to detect and quantify damages within the material, especially in the presence of nonlinear and non-Gaussian phenomena. Higher order statistics (HOS) such as bispectral analysis, can be seen as a decomposition of the third moment of a signal over frequency, and can be used to measure the magnitude of the even (second) order harmonic frequency components in the propagated ultrasonic waves [13]. Indeed, bispectrum is the two-dimensional Fourier Transform of the third order correlation function and is generally complex valued. For a real, zero-mean stationary random process $x(t)$, the power spectral density $P(\omega_m)$ and bispectrum $B(\omega_m, \omega_n)$ are given by [14]:

$$P(\omega_m) = \int_{-\infty-\infty}^{+\infty+\infty} R_{xx}(\tau) e^{j\omega_m \tau} d\tau \quad (1)$$

$$B(\omega_m, \omega_n) = \int_{-\infty-\infty}^{+\infty+\infty} R_{xxx}(\tau_1, \tau_2) e^{j(\omega_m \tau_1 + \omega_n \tau_2)} d\tau_1 d\tau_2 \quad (2)$$

where $R_{xx}(\tau)$ and $R_{xxx}(\tau_1, \tau_2)$ are the auto-correlation function and third order auto-correlation function of $x(t)$, respectively. By using the statistical expectation operator $E[\cdot]$, Eqs. (1) and (2) can be rewritten as:

$$P(\omega_m) = E[X(\omega_m)X^*(\omega_m)] \quad (3)$$

$$B(\omega_m, \omega_n) = E[X(\omega_m)X(\omega_n)X^*(\omega_m + \omega_n)] \quad (4)$$

where $X(\omega_m)$ is the Fourier Transform of the measured signal $x(t)$ and the asterisk sign “*” corresponds to a complex conjugate operation. Therefore, as the power spectrum decomposes the power of a signal, the bispectrum decomposes the third order cumulant by analysing the frequency interaction between the frequency components at ω_m , ω_n and $\omega_m + \omega_n$. However, due to several symmetries in the (ω_m, ω_n) plane, it is not necessary to compute $B(\omega_m, \omega_n)$ for all ω_m and ω_n pairs. Indeed, there exists a non-redundant region called the Principal Domain that is defined as [15]:

$$(\omega_m, \omega_n): 0 \leq \omega_m \leq \frac{2\pi f_s}{2}, \quad \omega_n \leq \omega_m, \quad 2\omega_m + \omega_n \leq 2\pi f_s \quad (5)$$

where f_s is the sampling frequency. In addition, the three frequency components ω_m , ω_n and $\omega_m + \omega_n$ have a special phase relation defined as follows:

$$\phi_k = \phi_m + \phi_n \quad (6)$$

where ϕ_m and ϕ_n are the phases of the signal at ω_m and ω_n , respectively, and ϕ_k is the phase of the signal at $\omega_m + \omega_n$. This last condition, known as quadratic phase coupling (QPC) [16], results from the second order nonlinearity due to structural damage, and it can be considered as the bispectrum's ability to detect nonlinear elastic features within the medium. In other words, if conditions (5) and (6) are satisfied, bispectral analysis can be significantly useful in sensing small high order nonlinear harmonic components induced by the interaction of elastic waves and the material defects. To this purpose, by setting $\omega_m = \omega_n = \omega_1$ and calculating the magnitude of Eqs. (3) and (4), yields:

$$|P(\omega_1)| = |X(\omega_1)X^*(\omega_1)| = |X(\omega_1)|^2 \quad (7)$$

$$|B(\omega_1, \omega_1)| = |X(\omega_1)X(\omega_1)X^*(\omega_1 + \omega_1)| = |X(\omega_1)X(\omega_1)X^*(\omega_2)| \quad (8)$$

with $\omega_2 = 2\omega_1$.

Estimation of Nonlinear Parameters

According to Landau's nonlinear classical theory [17] and Eq. (7), the standard second order nonlinear parameter β can be obtained as a solution of the nonlinear elastodynamic wave equation via a first order perturbation theory as follows [18]:

$$\beta_i(x, y) \propto \frac{\sqrt{|P(\omega_2)|}}{|P(\omega_1)|} \quad (9)$$

where $|P(\omega_2)|$ is the magnitude of the power spectral density associated with the second harmonic frequency component (i represents the transmitter position, (x, y) are the coordinates of a point over the top surface of panel). The parameter β is herein introduced to quantify the second nonlinear elastic response of a structure subjected to sinusoidal excitation. An analogous nonlinear parameter can be obtained from the bispectral analysis in order to measure the amount of coupling between the angular frequencies ω_1 and $2\omega_1$. In particular, the bicoherence b^2 is a useful normalized form of bispectrum that measures QPC on an absolute scale between 0 and 1 and can be defined as:

$$b_i^2(x, y) = \frac{|B(\omega_1, \omega_1)|^2}{P(\omega_1)P(\omega_1)P(\omega_2)} \quad (10)$$

Since the bispectrum has a variance proportional to the triple product of the power spectra, it can result in the second order properties of the acquired signal dominating the estimation. The advantage of normalisation is to make the variance approximately flat across all frequencies. Hence, both the parameter β and the bicoherence b^2 will be used to characterise the nonlinearity of the structural response of the composite laminate subjected to a harmonic excitation.

Visualization of the results

The results of the performed acquisitions have been post-processed through two different techniques: the first one is based on the simple visualization of the non-linear parameters before mentioned; the second one is based on the radial basis functions approach.

1. Nonlinear Imaging Technique

In this study a diagnostic nonlinear imaging method was developed to detect the second order nonlinear response of a damaged composite laminate using two sensors in pitch-catch mode. Both the second order nonlinear parameter β and the bicoherence coefficient b^2 were used to measure the second order nonlinear elastic effects due the interaction of the elastic waves with the crack interfaces (i.e. due to “clapping motion”) [19]. In particular, the damaged zone (i.e. the area on the top surface examined by the receiver sensor, with dimensions 210 mm x 150 mm) surrounding the defect was divided in $N = 5 \times 7$ cells distributed along a grid at intervals of 30 mm (Fig. 1).

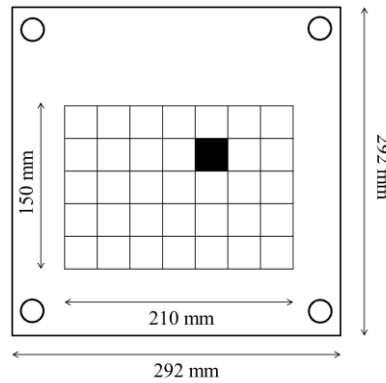


Figure 1. Representation of the damaged zone on the composite panel. The black square corresponds to the damage location. The circles represent the transmitter positions.

An excitation signals consisting of a 80-cycles, Hanning-windowed tone burst at 223.5 kHz was generated, amplified and used to drive a transmitter piezoelectric sensor surface bonded to the sample under investigation. Such a fundamental frequency was tuned to find local maxima in the sample response after a swept signal from 150 to 300 kHz, thus to fulfil the QPC condition [Eq. (6)]. The structural response was then acquired using a receiver piezoelectric sensor in each of the n ($1 \leq n \leq N$) cells of the damaged zone. According to Eqs. (9) and (10) both values of β and b^2 were calculated and plotted on a 2D map for each cell of the grid. As the transmitter sensor was moved on four different positions of the composite plate, four different maps were obtained and summed to retrieve the maxima of the nonlinear coefficients at the damage location:

$$\beta(x, y) = \sum_i^M \beta_i(x, y)$$

$$b^2(x, y) = \sum_i^M b_i^2(x, y)$$

where M is the number of transmitter positions (4 in this case).

2. Radial basis functions

Radial basis functions (RBF) are commonly used for scattered data interpolations problems, since they are able to interpolate arbitrary sets of point clouds in a smooth manner. This method is equally applicable to structured or unstructured grids, as well as poor quality meshes. Let us consider a set of points $\{\mathbf{r}_i\}_{i=1}^N \in \Omega \subset \mathfrak{R}^n$, with Ω the influence domain and $\mathbf{r}_i = x_i \hat{i} + y_i \hat{j}$. Let ϕ be a fixed, real-valued, radially symmetric function on \mathfrak{R}^n . Radial basis function interpolation method employs a “radial” function $\phi: \mathfrak{R}^n \rightarrow \mathfrak{R}$ to construct the interpolant scalar function $s(\mathbf{r})$, i.e the *radial basis function* of the form:

$$s(\mathbf{r}) = \sum_{i=1}^N \lambda_i \phi(\|\mathbf{r} - \mathbf{r}_i\|) + \sum_{j=1}^{N_{poly}} b_j p_j(\mathbf{r}) \quad (11)$$

where $p_j(\mathbf{r})$ is a basis for polynomials of degree at most k (typically linear or quadratic), $\|\mathbf{r} - \mathbf{r}_i\| = [(x - x_i)^2 + (y - y_i)^2]^{1/2}$ is the Euclidean norm so that $\phi\|\mathbf{r} - \mathbf{r}_i\|$ is the *basis function* centred at \mathbf{r}_i (in which the values are known), and λ_i and b_j are the weights or the expansion coefficients of the basis functions and the polynomial, respectively. N and N_{poly} denote the number of control points \mathbf{r}_i and the number of polynomial terms, with $N > N_{poly}$.

The RBF [Eq. (11)] consists of a weighted sum of a radially symmetric basis function ϕ located at the centres \mathbf{r}_i and a low degree polynomial $p_j(\mathbf{r})$. Given a set on N control points \mathbf{r}_i and values $\{f_i\}_{i=1}^N \subset \mathfrak{R}$, the process of finding an interpolating RBF $s(\mathbf{r})$ for any internal point m ($m=1, \dots, M$) of the mesh is called fitting and is given by:

$$s(\mathbf{r}) = \mathbf{M}^T \boldsymbol{\lambda} + \mathbf{P}^T \mathbf{b} \quad (12)$$

or

$$s(\mathbf{r}) = \mathbf{H}^T \mathbf{X} \quad (13)$$

where:

$$\begin{aligned}
\boldsymbol{\lambda} &= [\lambda_1, \lambda_2, \dots, \lambda_N]^T \quad [N \times 1] \\
\mathbf{b} &= [b_1, b_2, \dots, b_{N_{poly}}]^T \quad [N_{poly} \times 1] \\
\mathbf{M} &= \phi \|\mathbf{r} - \mathbf{r}_i\| \quad [N \times 1] \\
\mathbf{P} &= \begin{bmatrix} p_1 & p_2 & \cdots & p_{N_{poly}} \end{bmatrix} \quad [N_{poly} \times 1]
\end{aligned} \tag{14}$$

Assuming $\mathbf{P} = \begin{bmatrix} 1 & x & y & z \end{bmatrix}$, the vectors \mathbf{H} and \mathbf{X} become:

$$\begin{aligned}
\mathbf{H} &= [\phi \|\mathbf{r} - \mathbf{r}_1\| \quad \phi \|\mathbf{r} - \mathbf{r}_2\| \quad \cdots \quad \phi \|\mathbf{r} - \mathbf{r}_N\| \quad 1 \quad x \quad y \quad z] \\
\mathbf{X} &= [\lambda_1 \quad \lambda_2 \quad \cdots \quad \lambda_N \quad b_1 \quad b_2 \quad b_3 \quad b_4]^T
\end{aligned} \tag{15}$$

The coefficients λ_i and b_j in Eq. (11) are determined by enforcing the interpolation pass through all N scattered nodal points within the influence domain Ω

$$s(\mathbf{r}_i) = f_i \quad i = 1, \dots, N \tag{16}$$

Although the addition of polynomial terms does not improve greatly the accuracy for non-polynomial functions, theoretically studies revealed that there was not guarantee that the interpolating condition could be satisfied without the need of polynomial terms. The fitted RBF is defined by the coefficients of the basic function in the summation, together with the coefficients of the polynomial term $p_j(\mathbf{r})$. The most popular choices of ϕ are reported in [12]. RBF are very effective for interpolating scattered data as the associated system of linear equations is guaranteed to be invertible under very simple conditions on the locations of the data points. For instance, Gaussian and multiquadric radial basis functions place no restrictions on the locations of the points. Moreover, the thin-plate spline is more known a “*smoothest*” interpolator in the sense that not only it provides C^1 continuity¹ and satisfies the interpolation condition [Eq. (16)], but also it minimises certain energy functional. Particularly, given a set of nodes \mathbf{r}_i and a set of functions f_i , the thin-plate spline is the function $s^*(\mathbf{r})$ that satisfies the interpolator condition $s^*(\mathbf{r}_i) = f_i$ and minimises the integral of the second order derivative squared defined by:

$$s^* = \arg \min \|s\|$$

where

$$\begin{aligned}
\|s(\mathbf{r})\|^2 &= \int_{\mathbb{R}^3} \left(\frac{\partial^2 s(\mathbf{r})}{\partial x^2} \right)^2 + \left(\frac{\partial^2 s(\mathbf{r})}{\partial y^2} \right)^2 + \left(\frac{\partial^2 s(\mathbf{r})}{\partial z^2} \right)^2 \\
&+ 2 \left(\frac{\partial^2 s(\mathbf{r})}{\partial x \partial y} \right)^2 + 2 \left(\frac{\partial^2 s(\mathbf{r})}{\partial x \partial z} \right)^2 + 2 \left(\frac{\partial^2 s(\mathbf{r})}{\partial y \partial x} \right)^2 d\mathbf{r}
\end{aligned} \tag{17}$$

and $\|s(\mathbf{r})\|^2$ is a measure of the energy in the second order derivative of $\|s(\mathbf{r})\|$. Moreover, in order to ensure a unique solution of the resulting system of linear equations, the following orthogonality or side condition must be satisfied:

$$\sum_{i=1}^N x_i \lambda_i = \sum_{i=1}^N y_i \lambda_i = \sum_{i=1}^N z_i \lambda_i = 0 \tag{18}$$

More generally, if the polynomial in Eq. (11) is of degree m , then the side conditions imposed on the coefficients are

$$\sum_{i=1}^N \lambda_i q(\mathbf{r}_i) = 0 \tag{19}$$

for all polynomials q of degree at most m . Eqs. (16) and (19) lead to a linear system to solve for the coefficients that specify the RBF:

¹ The notation C^i is used to denote a function which is continuous in its first i derivatives

$$\begin{bmatrix} \mathbf{A} & \mathbf{P} \\ \mathbf{P}^T & \mathbf{0} \end{bmatrix} \begin{bmatrix} \boldsymbol{\lambda} \\ \mathbf{b} \end{bmatrix} = \begin{bmatrix} \mathbf{f} \\ \mathbf{0} \end{bmatrix} \quad (20)$$

or

$$\mathbf{GX} = \mathbf{Q} \quad (21)$$

where:

$$\mathbf{A} = \phi \|\mathbf{r}_i - \mathbf{r}_j\| \quad [N \times N]$$

$$\mathbf{P} = \begin{bmatrix} 1 & x_1 & y_1 & z_1 \\ 1 & x_2 & y_2 & z_2 \\ \vdots & \vdots & \vdots & \vdots \\ 1 & x_N & y_N & z_N \end{bmatrix} \quad [N \times N_{poly}] \quad (22)$$

and the vector of function values at each node is:

$$\mathbf{f} = [f_1, f_2, f_3, \dots, f_N]^T \quad [N \times 1] \quad (23)$$

Unique solution of Eq. (21) is obtained if the inverse of matrix \mathbf{G} exists:

$$\mathbf{X} = \mathbf{G}^{-1} \mathbf{Q} \quad (24)$$

Hence, the values f_m in each of the M points of the mesh with coordinates \mathbf{r} obtained through an interpolation with RBF, can be derived by substituting Eq. (24) in Eq. (13) as follows:

$$s(\mathbf{r}) = \mathbf{H}^T \mathbf{G}^{-1} \mathbf{Q} \quad (25)$$

3. EXPERIMENTAL SET-UP

The experiments were carried out on a composite carbon fibre reinforced plastic (CFRP) plate with dimensions 292 x 292 x 3 mm (Fig. 2). Stacking sequence and mechanical properties were not provided.

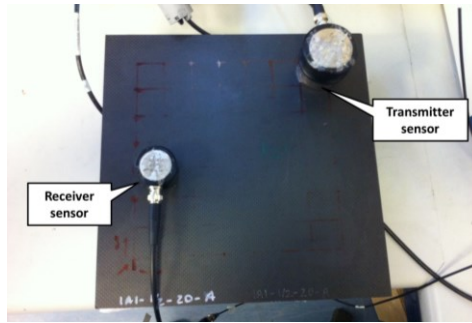


Figure 2. Composite test sample and piezoelectric transducers used in the experiments

To simulate delamination damage, the specimen was fabricated with a 10-mm squared Teflon patch inserted between the plies. The location of the damage was at coordinate $x = 135$ mm and $y = 105$ mm within the damaged zone with the origin at the left bottom corner of the grid (Fig. 1). To transmit the waveforms, a 50-mm-diameter Olympus – Panametrics NDT X1020 piezoelectric sensor with a central frequency of 100 kHz was surface bonded on the composite structure using a coupling gel. The transducer was linked to a preamplifier and connected to a National Instrument (NI) data acquisition system consisting of the NI PXI 5421 16-bit arbitrary waveform generator card to send the tone burst at 223.5 kHz. The excited voltage applied was around 250 V in order to maximize the efficiency of the available transducers. In order to measure the material nonlinear response, a 3-cm-diameter Olympus – Panametrics NDT V101

piezoelectric sensor with a central frequency of 500 kHz was connected to the NI PXI-5105 8-channel digitizer/oscilloscope card (Fig. 3).

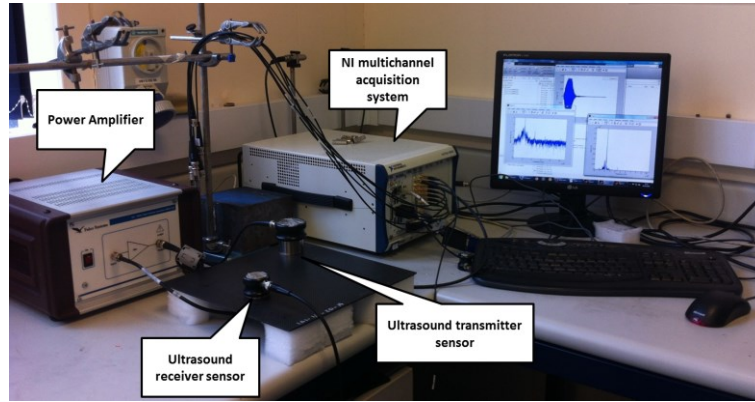


Figure 3. Experimental Set-up

The waveforms acquired in each cell of the damaged zone were averaged 20 times to reduce Gaussian noise and the uncertainties contained in the signals due to the coupling of the receiver sensor with the composite structure. Each nonlinear response was sampled at 20 MHz with a total acquisition time of 2 ms and then passed to a PC. Fig. 4 reports the time history and the associated spectrum of two measured signals, i.e. at the damage location (4c-d) and in a point far from it (4a-b). Whilst the presence of the second harmonic is clearly visible in both signals, its magnitude at the damage location is higher.

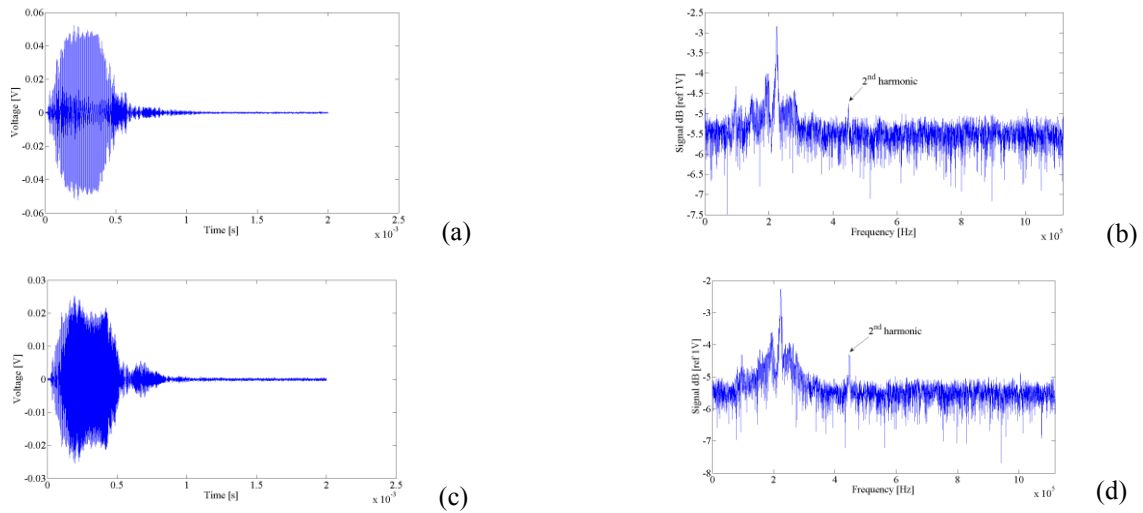


Figure 4. Time history and associate Fourier transform measured at coordinates $x = 15$ mm, $y = 15$ mm (4a-b) and at the damage location ($x = 135$ mm, $y = 105$ mm) (4c-d).

4. RESULTS

The acquired signals have been used to obtain an image representative of the damage conditions using the two different approaches for visualization before discussed.

First the envelope of the structural response was computed using the Hilbert transformation and, according to Eqs. (9) and (10), the damage location was retrieved through a 2D map of the values of β and b^2 for each cell of the damaged zone. Then, the transmitter sensor was moved in four different positions on the composite plate (outside the damaged zone) so that four different maps for both nonlinear coefficients were obtained. Fig. 5 represents the resulting 2D map of

the damage location accomplished by summing all four contributions of the nonlinear coefficients at each transmitter position. The maxima are deduced from the values nearest to 1.

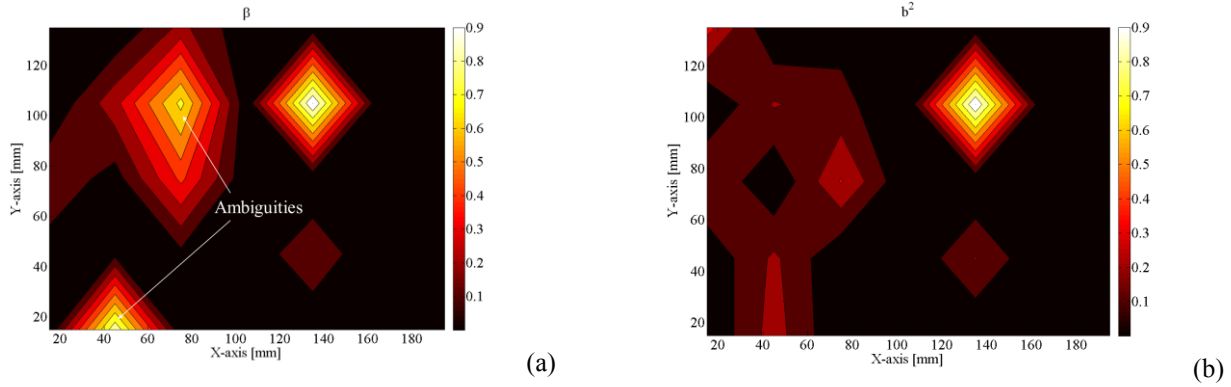


Figure 5. Image of the structural damage using the second order nonlinear coefficient β (a) and the bicoherence coefficient b^2 (b).

As it can be seen from Fig. 5, the bicoherence coefficient appeared to be very sensitive to the presence of the second order nonlinearities and, compared to the β parameter, it allowed obtaining a better estimation of the damage location. This might be due to the lack of information provided by the quadratic phase coupling between the fundamental and the second harmonic for the calculation of the second order nonlinear coefficient, which may lead to ambiguities in the image of the nonlinear source. Such ambiguities can be due to spurious experimental sources of nonlinearity such as the amplifier and the excitation transducer caused by the high input amplitude, which would be really difficult to be quantified. However, the bicoherence was able to reveal the presence of delamination (Teflon patch) within the composite laminate without the need of further signal processing to remove those undesired effects. Moreover, compared to other ultrasonic Guided Waves damage detection techniques, such an imaging process requires a simple signal processing to locate the nonlinear source as well as it does not need a priori knowledge of the mechanical properties, dispersion behaviour and a baseline with the undamaged structure.

The second visualization technique based on RBF has been then adopted. The following four different plots in Fig. 6 were achieved using a combination of RBF and the bicoherence coefficients (no ambiguities due to spurious experimental sources of nonlinearity).

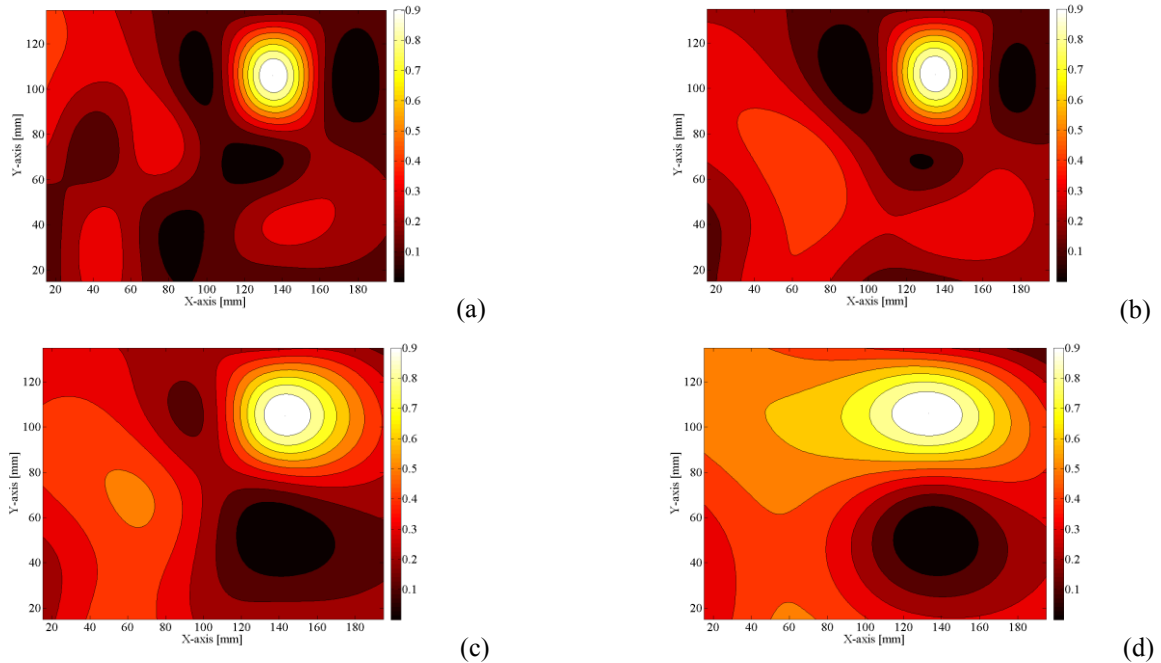


Figure 6. Image of the structural damage using the the bicoherence coefficient b^2 post-processed through RBF using – (a) 35 points; (b) 20 points; (c) 10 points; (d) 6 points.

In all the cases the 2D map was retrieved as a sum of the RBF contribution of four different transmitter positions. For the RBF implementation, the number of points was decreased from the total 35 points to 20, 10 and only 6 points. In all cases the position of the damage location was achieved with high level of accuracy. It is worth to be noted that the last three figures the point associated with the damage was not included for the RBF evaluation.

The main conclusion that can be drawn from the Fig. 6 is that RBF is effective in damage representation also using a limited sparse net of points of acquisitions over the top surface of the panel. As it can be expected, limiting the number of points, the predicted extent of the damage increases since less information lead to a higher degree of uncertainty resulting in a more extended area on the sample in which the damage could be located. Nevertheless, in each case the visualization technique provides useful and correct results since the actual damage is always included in the predicted area. RBF approach can be therefore considered able to represent and to localize the damage properly but with a degree of accuracy, concerning the extent of the area enclosing it, sensitive to the number of employed acquisition points.

5. CONCLUSIONS

The paper presents the experimental results concerning a state of art technology for the detection and localization of damage in composite structures. The basic principle is that the level of nonlinearity in the elastic response of materials containing structural damage is far greater than in materials with no structural damage. Indeed, nonlinear wave diagnostics of damage are remarkably sensitive to the detection and progression of damage in materials. Nonlinear wave modulation spectroscopy (NWMS) is one exemplary method in this class of dynamic nondestructive evaluation techniques. The sample adopted for the experimental tests was a square composite panel typical for aerospace applications inside which a patch has been inserted to simulate damage conditions: exciting this sample with a sine burst properly chosen, the spectral data have demonstrated a strong nonlinearity essentially represented by the occurrence of the second harmonic related to the fundamental frequency component. Undamaged materials are essentially linear in their response, therefore this spectral property reveals the presence of a structural damage (the patch). Time signals have been post-processed to obtain bispectrum and bicoherence in the different locations of the acquisition grid and to visualize on the sample the spectral statistics. RBF approach has been found very suitable for visualizing the damage on the sample also using a limited number of acquisition points. The activities have shown that both the adopted indicators allowing for the exact damage localization but, indeed, the bicoherence, in this case, appears the most suitable.

REFERENCES

- [1] Ray, B.C., Hasan, S.T., Clegg, D.W., "Evaluation of Defects in FRP Composites by NDT Techniques," *Journal of Reinforced Plastics and Composites*, (2007), 26:1187-1192.
- [2] Salawu, O. S., "Detection of structural damage through changes in frequency: a review," *Eng. Struct.* 9:718–23 (1997).
- [3] Scarselli, G., Maffezzoli, A., Castorini, E., Taurino, A., "Vibrational analysis of aerospace composite components for production defects and operating damage detection," *Proceedings of 9th International Conference on Composite Science and Technology (ICCST9)*, 811-819, (2013).
- [4] Abeele, K.E.-A. VD, Sutin, A., Carmeliet, J., Johnson, P. A., "Micro-damage diagnostics using nonlinear elastic wave spectroscopy (news)," *NDT&E. Int.* 34:239–48, (2001).
- [5] Amura, M., Meo, M., "Prediction of residual fatigue life using nonlinear ultrasound," *Smart Materials and Structures*, (2012), 21 (4), 045001.
- [6] Zaitsev, V., Sas, P., "Nonlinear response of a weakly damaged metal sample: a dissipative modulation mechanism of vibro-acoustic interaction," *J. Vib. Control.* 6:803–22 (2000).
- [7] Kyung-Young Jhang, "Applications of Nonlinear Ultrasonics to the NDE of Material Degradation," *IEEE transactions on ultrasonics, ferroelectrics, and frequency control* 47(3):540–8, (2000).
- [8] Meo, M., Zumpano, G., "Nonlinear elastic wave spectroscopy identification of impact damage on a sandwich plate," *Composite Structures*, 71: 469–474, (2005).
- [9] Zumpano, G., Meo, M., "Damage localization using transient non-linear elasticwave spectroscopy on composite structures," *International Journal of Non-Linear Mechanics*, 43: 217 – 230, (2008).

- [10] Van Den Abeele, K. E.-A., Johnson, P. A., Sutin, A., "Nonlinear ElasticWave Spectroscopy (NEWS) Techniques to Discern Material Damage, Part I: Nonlinear Wave Modulation Spectroscopy (NWMS)," *Res. Nondestr. Eval.*, 12:17–30, (2000).
- [11] Ciampa, F., Meo, M., "Nonlinear elastic imaging using reciprocal time reversal and third order symmetry analysis," *J. Acoust. Soc. Am.* 131 (6), 4316-4323, (2012).
- [12] Carr, J. C., Beatson, R. K., Cherrie, J. B., Mitchell, T. J., Fright, W. R., McCallum, B. C, Evans, T. R., "Reconstruction and Representation of 3D Objects with Radial Basis Functions," *SIGGRAPH' 01, Proceedings of the 28th annual conference on Computer graphics and interactive techniques*, 67-76.
- [13] Kim, Y.-C., Powers, E.-J., "Digital Bispectral Analysis and its Applications to Nonlinear Wave Interactions," *IEEE Transactions on Plasma Science*, Ps-7, 120-131 (1979).
- [14] Fackrell, J.W.-A., White, P.-R., Hammond, J.-K., Pinnington, R.-J., Parson, A.-T., "The Interpretation of the Bispectra of Vibration Signals: Part 1: Theory," *Mechanical systems and Signal Processing*, Vol. 9, No. 3, 257-266 (1995).
- [15] Nikias, C.-L., Raghuveer, M.-R., "Bispectrum estimation: a digital signal processing framework," *Proc. IEEE* 75, 869-91 (1987).
- [16] Fackrell, J. W.-A., McLaughlin, S. "The Higher Order Statistics of Speech Signals," *Proceedings of the IEE Colloquium on Techniques in Speech Signal Processing*, London, Digest No. 1994/138, 7/1-7/6 (1994).
- [17] Landau, L. D., Lifshitz, E. M., [Theory of Elasticity], Chap. III, Pergamon, Oxford, (1986).
- [18] L. Ostrovsky, P.-A. Johnson. "Dynamic nonlinear elasticity in geomaterials," *Riv. Nuovo Cim.* 24, 1–46 (2001).
- [19] Pecorari, C., "Nonlinear interaction of plane ultrasonic waves with an interface between rough surfaces in contact," *J. Acoust. Soc. Am.* 113 (6), 3065-72 (2003).